Optimization-based reduction of contour errors of heavy plates in hot rolling

authored by **F. Schausberger, A. Steinböck, and Kugi**

and published in *Journal of Process Control*.

Automation and Control Institute (ACIN)
TU Wien
Gusshausstrasse 27-29/E376
1040 Vienna, Austria

Internet: www.acin.tuwien.ac.at
E-mail: office@acin.tuwien.ac.at
Phone: +43 1 58801 37601
Fax: +43 1 58801 37699

Optimization-based reduction of contour errors of heavy plates in hot rolling

F. Schausberger*, A. Steinboeck, A. Kugi

Automation and Control Institute, TU Wien, Gußhausstraße 27–29, 1040 Vienna, Austria

Abstract

This paper deals with the reduction of top view contour errors in the hot rolling process. Deviations between the actual plate contour and the desired shape may result from asymmetric rolling conditions caused by, e.g., temperature gradients or non-homogeneous input thickness profiles. Under real rolling conditions these disturbances are hard to predict and hence cannot be compensated in a feedforward approach. Therefore, it seems suitable to apply feedback when contour errors occur. This approach essentially requires a measurement of the plate contour and a mathematical model to predict the plate contour after the roll pass. This model is the basis for an optimization-based approach to determine the necessary adjustment of the rolling mill to reduce contour errors. The optimization problem allows to systematically incorporate constraints on the asymmetry of the output plate thickness. Generally, the compliance of the mill stand is not strictly symmetric and may deteriorate the result of the presented approach. The asymmetric compliance results in an asymmetric deflection of the mill stand which is compensated in an empirical approach utilizing the forces applied during the roll pass. Simulation results and measurements of plates rolled during the normal production demonstrate the effectiveness of the proposed method.

Keywords: Shape control of heavy plates, Heavy plate mill, Unconstrained optimization, Model-based control, Model-based estimator, Snaking

1. Introduction

1.1. Shape control in hot rolling

In steel-mills, the thickness of heavy plates is successively reduced to a desired final plate thickness using heavy plate mills (cf. Fig. 1). The term roll pass or pass denotes a single reduction of the thickness of the plate, which is typically performed in alternating direction at reversing mill stands. Beside the material properties and the thickness homogeneity of the plate, the quality of the plate is mainly characterized by the shape after the last roll pass. In general, the shape of the plate, as seen in top view, should be rectangular to maximize the usable area. During the rolling process deviations from the desired plate shape may occur, which is called camber. This may cause a lowered product quality, product rejects, and in the worst case even damaged plant components downstream of the rolling mill. The deviations may result from asymmetric conditions during the rolling process, e.g., non-homogeneous temperature or thickness distributions in the lateral direction.

The asymmetric rolling conditions are generally unknown and cannot be compensated in advance to prevent the plate from cambering. Therefore, a common approach is to apply feedback if a shape defect occurs. Clearly, this requires the measurement of the contour of the plate. A plate with a camber before the roll pass may lead to an off-center position of the plate in the lateral direction. The consequences are asymmetric rolling forces and a non-homogeneous rolling gap which may further increase camber. This implies that the contour and the lateral position of the plate should be measured during the roll pass. To determine the necessary control input of the mill stand, the evolution of the plate contour must be thoroughly understood. The literature offers several approaches to model the evolution of the plate contour in hot rolling, see, e.g., [1; 2; 3; 4; 5; 6]. They differ widely in terms of accuracy and computational effort, ranging from simple models only utilizing the continuity of mass in the roll gap to finite-element-method (FEM) simulations covering complex models of the rolled material and the mill stand.

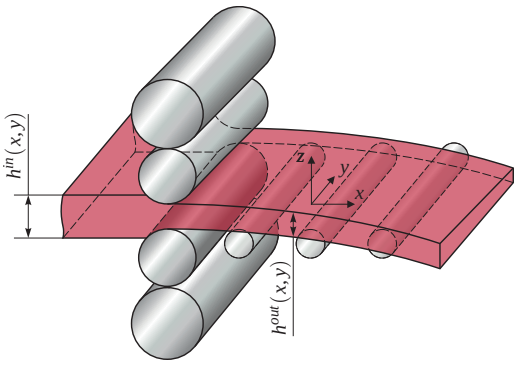

Figure 1: 4-high rolling mill and heavy plate with a contour error.

*Corresponding author. *Tel.:* +43 1 58801 376231, *fax:* +43 1 58801 9376231.

Email addresses: schausberger@acin.tuwien.ac.at (F. Schausberger), andreas.steinboeck@tuwien.ac.at (A. Steinboeck), kugi@acin.tuwien.ac.at (A. Kugi)

Post-print version of the article: F. Schausberger, A. Steinböck, and Kugi, "Optimization-based reduction of contour errors of heavy plates in hot rolling", *Journal of Process Control*, vol. 47, pp. 150–160, 2016, ISSN: 0959-1524. DOI: 10.1016/j.jprocont.2016.09.010
The content of this post-print version is identical to the published paper but without the publisher's final layout or copy editing.

Nomenclature

Latin symbols

$\bar{h}$	center-thickness of the plate
A, **b**	system of linear equations
c	polynomial coefficient vector of the plastic strain
d	search direction
e	vector of the quadratic objective function
H	Hessian
J	Jacobian
a_i	polynomial coefficient of the quadratic interpolation
$c_{i,k}$	polynomial coefficient of the plastic strain
E	Young's modulus
F	Airy's stress function
F_{roll}	rolling force
G	shear modulus
h	thickness of the plate
k_F, k_B	compliance constants
l	length of the plate
M_{CL}	number of centerline grid points
N_P	number of asymmetry grid points
N_{PB}	degree of the boundary polynomials
P	penalty function
P_x	polynomial degree in x-direction
P_y	polynomial degree in y-direction
p_{Bi}	polynomial of the plate boundary
u	displacement in x-direction
V	objective function
v	displacement in y-direction
w	width of the plate
w_{cyl}	lateral distance between the cylinders of the roll gap actuator
x, y, z	Cartesian coordinates
x_i	grid point of the asymmetry of the plate
x_j	grid point of the centerline of the plate

Greek symbols

α	step size of the line search
β_i	weighting factor
Δh	asymmetry of the plate thickness
Δh_0	offset of the asymmetry of the mill stand
δ	centerline of the plate
δ_{max}	maximum lateral deviation of the centerline
ϵ	strain
γ_x, γ_V, γ_{dV}	tuning parameters of the optimization
κ	ratio between actual and required asymmetry
λ	weighting function
$\mathcal{R}$	residual
ν	Poisson's ratio
Ω	integration domain
ϕ	boundary value function in x-direction
ψ	boundary value function in y-direction
σ	stress
$\boldsymbol{\Delta h}$	vector of thickness asymmetries
$\boldsymbol{\lambda}$	vector of weighting functions

Operators

Δ	Laplacian
∇	Nabla

Subscripts

act	actual
CMD	contour measurement device
$comp$	compensation
des	desired
$dist$	disturbance
$estim$	estimated
hom	homogeneous
max	maximal
min	minimal
$part$	particular
ref	reference
req	required
xx	normal component in x-direction
xy	shear component
yy	normal component in y-direction

Superscripts

$*$	optimal
el	elastic
in	input
out	output
pl	plastic

1.2. Existing solutions

Several approaches to avoid contour errors and off-centering of the strip in tandem hot strip rolling may be found in the literature. In the hot strip rolling process, several consecutive mill stands are used to reduce the thickness of the strip. Contrary to configurations with reversing mill stands, the rolling direction does not change. Kiyota et al. (cf. [7]) derived a model covering the plastic deformation of the strip in the rolling gap and the elastic deformation of the mill housing. Based on a linear model of the movement of the plate, an optimal regulator and a state observer are designed and validated using simulations. Furthermore, adjustment coefficients accounting for different rolling conditions are introduced. Sliding mode control and a state observer are presented in [8] to reduce the lateral movement of the strip. The controller design is based on a linear mathematical model using the asymmetry of the roll gap as control input. Simulation and measurement results from an industrial plant show the achieved improvements. Also model

Post-print version of the article: F. Schausberger, A. Steinböck, and Kugi, "Optimization-based reduction of contour errors of heavy plates in hot rolling", *Journal of Process Control*, vol. 47, pp. 150–160, 2016, ISSN: 0959-1524. DOI: 10.1016/j.jprocont.2016.09.010
The content of this post-print version is identical to the published paper but without the publisher's final layout or copy editing.

predictive control (MPC) is used to reduce the lateral movement of strips in hot rolling (cf. [9]). The MPC formulation allows the systematic incorporation of input and state constraints in the design of the controller. A MIMO H_2 controller that is robust against heterogeneous properties of different rolled products is presented in [10]. Here, the tilt of several mill stands is used as control input. Simulation and experimental results show the effectiveness of the proposed method.

The reduction of contour errors during the rolling using reversing mill stands is only barely discussed in literature. An early control-based attempt to reduce the camber in plate rolling was presented in [11]. There, a model linking the thickness wedge with the contour of the plate as well as a setup to measure the camber of the plate are discussed. The term wedge denotes an asymmetric thickness profile of the plate in the lateral direction. Correction coefficients have to be manually tuned to achieve an appropriate model accuracy. The camber of the plate is measured in the forward pass whereas the asymmetry of the roll gap is only adjusted in the backward pass to reduce camber.

A FEM based simulator to predict camber in hot rolling was developed by Jeong et al. (cf. [12]). The plate is treated as a rigid perfectly plastic body in the three-dimensional problem formulation of the deformation in the roll gap. The developed FEM simulator is used to design an output feedback fuzzy controller for the camber and the lateral movement of the plate. The asymmetry of the roll gap is adjusted during the actual pass. The resulting controller is compared with a PI-controller utilizing the presented simulator.

1.3. Motivation and objectives of this work

In this work, camber control using a reversing mill stand is discussed. Here, the subsequent roll passes offer the use of two different control strategies:

- Measure the plate contour and counteract to contour errors during the same pass.
- Use the measurement of the plate contour to reduce the occurring camber in the subsequent pass(es).

Plates with camber may collide with and thus damage plant components downstream the rolling mill. If a large camber occurs, the first approach seems beneficial because camber is reduced earlier compared to the second one. However, there exists a time delay between the generation and the measurement of the plate contour. Hence, all appearing errors can only be corrected with a delay. This is why it also seems suitable to adjust the inputs of the mill stand in the next pass for the compensation of contour errors. Nevertheless, the second approach cannot eliminate contour errors appearing in the last pass.

Additionally to the top-view shape of the plate, especially the homogeneity of the plate thickness defines the quality of the final rolled plate. Hence, the effect of camber-reducing countermeasures on the thickness distribution of the plate should be considered in the controller design. The existing solutions to curb camber in the hot rolling of heavy plates only focus on one of the discussed control strategies. Also constraints on the maximum asymmetry of the thickness of the plate are not taken into account.

All these facts were the motivation to develop a new control strategy to curb camber in the hot rolling process fulfilling the following requirements:

- Counteract shape errors both in the actual pass and in consecutive passes.
- System constraints, e.g., the maximum asymmetry of the mill stand, can be systematically incorporated into the controller design.
- The control objective can be adjusted such that a reasonable contour is achieved and the demands on the thickness tolerances are fulfilled.

These requirements demand

- a precise measurement of the plate contour during the roll pass with a small time delay and
- an accurate mathematical model of the contour evolution with a moderate computational effort.

In this paper, an optimization-based approach is proposed that utilizes an accurate mathematical model of the contour evolution. This choice was made because input and system constraints can be systematically taken into account. Furthermore, the control objectives can be adjusted in an intuitive manner by shaping the objective function. The automation system of the considered rolling mill only allows to change the desired asymmetry of the output thickness before the roll pass and therefore no adjustment of the thickness profile is possible during the roll pass. Hence, the presented method for the reduction of camber is only applied to the second control strategy. However, the methods being presented are also applicable to the first control strategy.

A graphical overview of the approach to reduce camber is shown in Fig. 2. The measurements of an infrared camera are utilized to determine the contour of the plate. The measured contour after the pass is used in combination with a mathematical model of the contour evolution to determine the necessary adjustment of the roll gap actuators in the next pass to reduce contour errors.

1.4. Structure of the paper

The paper is organized as follows: In Section 2, a method to determine the contour presented in [13] is shortly summarized. A mathematical model of the contour evolution of the plate published in [14] is reviewed in Section 3. Based on this model, an optimization-based approach to reduce camber is presented in Section 4. An approach to compensate the asymmetric compliance of the mill stand can be found in Section 5, and simulation results of the proposed method are given in Section 6. The implementation of the control strategy is discussed in Section 7. Furthermore, the feasibility of the proposed method is demonstrate by means of measurements from an industrial plant. Section 8 contains a short summary and gives an outlook on future research activities.

Post-print version of the article: F. Schausberger, A. Steinböck, and Kugi, "Optimization-based reduction of contour errors of heavy plates in hot rolling", *Journal of Process Control*, vol. 47, pp. 150–160, 2016, ISSN: 0959-1524. DOI: 10.1016/j.jprocont.2016.09.010
The content of this post-print version is identical to the published paper but without the publisher's final layout or copy editing.

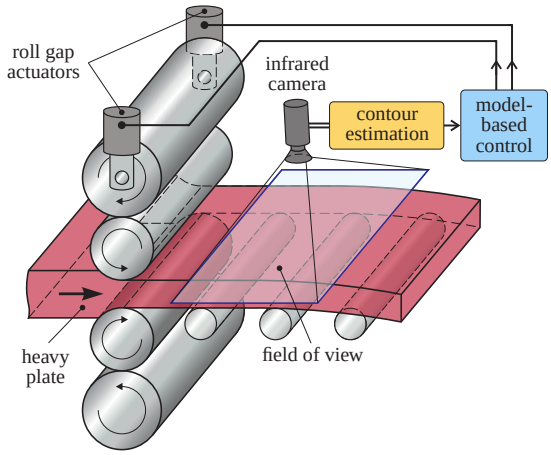

Figure 2: Overview of the camber reducing control approach.

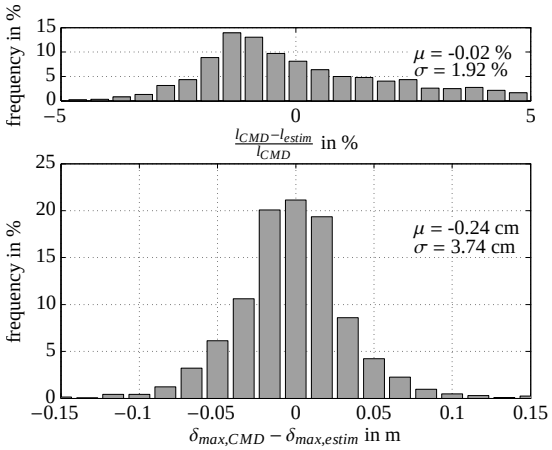

Figure 3: Frequency distribution in terms of maximum lateral deviation δ_{max} and length of the plate l.

2. Estimation of the plate contour

Besides a precise mathematical model of the contour evolution, the measurement of the actual plate contour is an important aspect of the presented method for the reduction of camber. Here, the longitudinal edges as well as the shape of the head and tail end of the plate are of interest. The head contour of the plate is the first lateral edge leaving the roll gap, whereas the tail end passes the roll gap at the end of the pass. An infrared camera is installed before and after the considered rolling mill to measure the contour of the plate in both rolling directions. In general, the whole plate cannot be captured within a single image because the plate is typically too long and partly hidden by other plant components. Hence, the camera only captures parts of the rolled plate and the contour has to be determined based on several consecutive images. In [13], the edges of the plate within a single image are determined using an edge detection algorithm. The result of the edge detection is then fed into an optimization-based algorithm which yields the whole contour of the plate. The presented approach utilizes the restrictions of the plate movement resulting from the plate being clamped in the roll gap. Additionally, the algorithm estimates the movement of the plate characterized by its angular and longitudinal velocity. Furthermore, the lateral position of the plate in the roll gap is estimated which facilitates the adjustment of the roll gap actuators to compensate asymmetric loads caused by the off-centering of the plate. The contour estimation yields the boundary contour as a series of boundary points defined in a Cartesian coordinate system.

The contour measurement is installed at the finishing mill of AG der Dillinger Hüttenwerke, Germany. Here, the developed measurement system has proven to be robust against the harsh conditions at the rolling mill for the last two years and without any maintenance. In Fig. 3, the results of the contour estimation system (Index estim) are compared with those of a contour measurement device (Index CMD) located at the end of the processing line. For this comparison, the lateral deviation δ_{max} of the centerline of the plate as shown in Fig. 4 and the plate length l are used.

The large distance between the CMD and the mill stand makes it impossible to use the CMD for feedback to reduce contour errors. The statistics shown in Fig. 3 covers more than 3000 plates which where rolled within two months and which had a minimum length of 20 m. Shorter plates are not considered because camber does not play an important role for these plates. The upper part of Fig. 3 shows the frequency distribution of the relative error of the estimated length l of the plates and the frequency distribution of the maximum lateral deviation δ_{max} is depicted in the lower part. The latter histogram agrees well with a symmetrical normal distribution with over 90 percent of the measurements featuring an error of less than 5 cm.

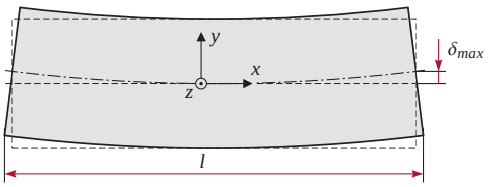

Figure 4: Definition of the maximum lateral deviation δ_{max} and the length of the plate l.

3. Modeling of the evolution of the plate contour

The basis for the proposed method to reduce camber in hot rolling is a suitable mathematical model of the contour evolution. In this work, a continuum-mechanics-based model of the contour evolution presented in [14] is used. This model was chosen because it features an accurate prediction of the contour evolution and a moderate computational effort.

A schematic of the rolling process with the input thickness $h^{in}(x,y)$ and the output thickness $h^{out}(x,y)$ is shown in Fig. 1. As indicated in this figure, a Cartesian coordinate system with coordinates x, y, and z is used. It is assumed that any plastic deformation of the plate occurs inside the roll gap. This implies that the residual stresses induced during the roll pass do not

Post-print version of the article: F. Schausberger, A. Steinböck, and Kugi, "Optimization-based reduction of contour errors of heavy plates in hot rolling", *Journal of Process Control*, vol. 47, pp. 150–160, 2016, ISSN: 0959-1524. DOI: 10.1016/j.jprocont.2016.09.010
The content of this post-print version is identical to the published paper but without the publisher's final layout or copy editing.

exceed the yield strength of the rolled material. Furthermore, no lateral expansion of the plate is considered. With a known input and output thickness, the plastic strain in the longitudinal direction x reads as

$$\epsilon_{xx}^{pl} = \frac{h^{in}(x,y)}{h^{out}(x,y)} - 1, \tag{1}$$

where x and y are Lagrangian coordinates. That is the coordinates are fixed with the material points.

The model uses the plastic deformation (1) and the contour of the plate before the rolling pass to predict the contour after the rolling pass by means of the displacements $u(x,y)$ and $v(x,y)$ of the plate in the longitudinal and lateral direction, respectively. The model of [14] is very briefly revisited in the following. It will be used in Section 4 in the optimization-based control concept to reduce occurring camber.

3.1. Mathematical model

The deformation problem is considered as two-dimensional (directions x and y), because non-uniformities along the coordinate z are assumed to be negligible. Moreover, a plane state of stress is assumed. This assumption is supported by the small dimensions in the thickness direction compared to the width and length of the plate and the absence of surface tractions (cf. [15]). These assumptions facilitate the calculation of the residual stresses and strains in the plate. The equilibrium equations for the considered two-dimensional problem read as

$$\frac{\partial \sigma_{xx}}{\partial x} + \frac{\partial \sigma_{xy}}{\partial y} = 0 \tag{2a}$$

$$\frac{\partial \sigma_{xy}}{\partial x} + \frac{\partial \sigma_{yy}}{\partial y} = 0, \tag{2b}$$

with the shear stress σ_{xy} and the normal stresses σ_{xx} and σ_{yy}. These residual stresses remain in the plate after the plastic deformation in the roll gap and the resulting elastic recovery. The residual stresses are linked with the elastic strains ϵ_{xx}^{el}, ϵ_{yy}^{el} and ϵ_{xy}^{el} by the constitutive equations

$$\epsilon_{xx}^{el} = \frac{1}{E}\left(\sigma_{xx} - \nu\sigma_{yy}\right), \tag{3a}$$

$$\epsilon_{yy}^{el} = \frac{1}{E}\left(\sigma_{yy} - \nu\sigma_{xx}\right), \tag{3b}$$

and

$$\epsilon_{xy}^{el} = \frac{1}{2G}\sigma_{xy}, \tag{3c}$$

which assume a linear elastic material behavior. Here, E denotes Young's modulus, G is the shear modulus and ν Poisson's ratio. The total strain in the plate is a superposition of elastic and plastic strain components in the form

$$\epsilon_\Lambda = \epsilon_\Lambda^{el} + \epsilon_\Lambda^{pl}, \quad \Lambda \in \{xx, xy, yy\}. \tag{4}$$

Additionally, the total strains are subject to the compatibility equation

$$\frac{\partial^2 \epsilon_{xx}}{\partial y^2} + \frac{\partial^2 \epsilon_{yy}}{\partial x^2} = 2\frac{\partial^2 \epsilon_{xy}}{\partial x \partial y}, \tag{5}$$

which guarantees a single-valued displacement field (cf. [15]). By insertion of (3) into (4) and further into (5) the continuum mechanics problem can be rewritten with $G = \frac{E}{2(1+\nu)}$ in the form

$$\begin{aligned}&\frac{\partial^2 \sigma_{xx}}{\partial x^2} + \frac{\partial^2 \sigma_{xx}}{\partial y^2} + \frac{\partial^2 \sigma_{yy}}{\partial x^2} + \frac{\partial^2 \sigma_{yy}}{\partial y^2} \\ &= -E\left(\frac{\partial^2 \epsilon_{xx}^{pl}}{\partial y^2} + \frac{\partial^2 \epsilon_{yy}^{pl}}{\partial x^2} - 2\frac{\partial^2 \epsilon_{xy}^{pl}}{\partial x \partial y}\right).\end{aligned} \tag{6}$$

The so called Airy's stress function $F(x,y)$, which is defined in the form

$$\sigma_{xx} = \frac{\partial^2 F}{\partial y^2}, \quad \sigma_{yy} = \frac{\partial^2 F}{\partial x^2}, \quad \sigma_{xy} = -\frac{\partial^2 F}{\partial x \partial y}, \tag{7}$$

and hence automatically fulfills (2), is used to solve (6). Utilizing $F(x,y)$, (6) can be formulated as fourth-order inhomogeneous partial differential equation

$$\Delta\Delta F = -E\left(\frac{\partial^2 \epsilon_{xx}^{pl}}{\partial y^2} + \frac{\partial^2 \epsilon_{yy}^{pl}}{\partial x^2} - 2\frac{\partial^2 \epsilon_{xy}^{pl}}{\partial x \partial y}\right), \tag{8}$$

with the Laplacian $\Delta = \frac{\partial^2}{\partial x^2} + \frac{\partial^2}{\partial y^2}$. Eq. (8) is also known as biharmonic equation. In the considered application, the stress function F has to fulfill the homogeneous boundary conditions (cf. [14]). I.e, the absence of surface tractions has to be ensured. Once a solution $F(x,y)$ is known, the residual stresses are calculated according to (7). The displacements u and v in the longitudinal and lateral direction between the contour before and after the roll pass are obtained by integrating the total strains (4), i.e.,

$$u(x,y) = \int_0^x \epsilon_{xx}^{el}(\bar{x},y)\mathrm{d}\bar{x} + \int_0^x \epsilon_{xx}^{pl}(\bar{x},y)\mathrm{d}\bar{x} + \frac{1}{E}\phi(y) \tag{9a}$$

and

$$v(x,y) = \int_0^y \epsilon_{yy}^{el}(x,\bar{y})\mathrm{d}\bar{y} + \int_0^y \epsilon_{yy}^{pl}(x,\bar{y})\mathrm{d}\bar{y} + \frac{1}{E}\psi(x), \tag{9b}$$

with scalar functions $\phi(y)$ and $\psi(x)$. They define the boundary values of the displacements, see [14].

3.2. Solution of the biharmonic equation

Searching for an analytical solution of (8) that satisfies the boundary conditions is difficult. Hence, a stress function in the form of a power series that automatically fulfills (8) but not necessarily the boundary conditions is used, cf. [14]. The linearity of (8) facilitates the superposition ansatz

$$F = F_{hom} + F_{part},$$

with F_{hom} as the solution of the homogeneous part of (8). The particular solution F_{part} satisfies the full equation (8) but does not necessarily meet the boundary conditions. Hence, F_{hom} is

Post-print version of the article: F. Schausberger, A. Steinböck, and Kugi, "Optimization-based reduction of contour errors of heavy plates in hot rolling", *Journal of Process Control*, vol. 47, pp. 150–160, 2016, ISSN: 0959-1524. DOI: 10.1016/j.jprocont.2016.09.010
The content of this post-print version is identical to the published paper but without the publisher's final layout or copy editing.

utilized to fulfill the boundary conditions. The plastic deformation (1) is approximated by a two-dimensional polynomial

$$\epsilon_{xx}^{pl} = \sum_{i=0}^{P_x} \sum_{k=0}^{P_y} c_{i,k} x^i y^k, \tag{10}$$

with the coefficients $c_{i,k}$, $i = 0,\dots,P_x$ and $k = 0,\dots,P_y$ and the degrees P_x and P_y in the longitudinal and lateral direction, respectively. The remaining plastic strains are set to $\epsilon_{yy}^{pl} = \epsilon_{xy}^{pl} = 0$ because zero lateral expansion of the plate in the rolling gap is assumed. Based on (10), F_{part} also follows as a power series. The terms of F_{part} can be individually determined by inserting each element of (10) into (8) because of the linearity of (8). Consequently, F_{hom} is also formulated as a power series whereas the coefficients are used to satisfy the boundary conditions in an approximate manner.

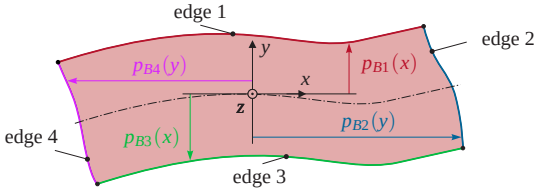

Figure 5: Parameterization of the plate boundary.

Moreover, it is necessary to parameterize each edge of the plate before the roll pass. A closed-form parameterization by polynomials p_{Bi}, $i = 1,\dots,4$, see Fig. 5, seems favorable because derivatives of the boundary representation are required for the calculations. The coefficients of the polynomials result from a least-squares approximation of the boundary points obtained by the contour estimation system.

4. Optimization-based reduction of contour errors

In this section, an optimization-based reduction of the camber of heavy plates is presented. To this end, the contour measurement described in Section 2 is used to determine the plate contour. Based on the mathematical model discussed in Section 3 and the measured contour, the required asymmetry of the output thickness to achieve the desired contour after the next pass is computed. The automation system of the considered rolling mill only allows to set the desired asymmetry of the output thickness before the roll pass and therefore no adjustment of the thickness profile is possible during the roll pass. This is why the calculation is performed once after every pass. However, the presented approach can also be applied to determine the adjustment of the rolling mill during the roll pass. Based on the required asymmetry to curb camber, the actuators of the roll gap (cf. Fig. 2) are adjusted using the subordinate automatic gauge control (AGC), see, e.g., [16]. Here, an ideal control of the roll gap profile is assumed, i.e. there exists no deviation between the required and the resulting asymmetry of the output thickness.

4.1. Parameterization of the thickness profiles

The automation system installed at the considered rolling mill allows to adjust the desired values of the center-thickness $\bar{h}^{out}$ and the asymmetry Δh^{out} of the output thickness on a regular spatial grid in the longitudinal direction of the plate. A linear interpolation is performed between the grid points. Consequently, the profile of the output thickness $h^{out}(x,y)$ is parameterized as

$$\begin{aligned} h^{out}(x,y) = \bar{h}_i^{out} &+ \frac{\bar{h}_{i+1}^{out} - \bar{h}_i^{out}}{x_{i+1} - x_i}(x - x_i) \\ &+ \frac{y}{w}\left[\Delta h_i^{out} + \frac{\Delta h_{i+1}^{out} - \Delta h_i^{out}}{x_{i+1} - x_i}(x - x_i)\right] \\ \forall\ x_i \le x \le x_{i+1}, &\ 1 \le i \le N_P - 1 \end{aligned} \tag{11}$$

with the grid points x_i, $i = 1,\dots,N_P$ and the plate width w. The center-thickness $h^{out}(x,0)$ may be adjusted by the coefficients $\bar{h}_i^{out}$, $i = 1,\dots,N_P$, whereas the coefficients Δh_i^{out} vary the asymmetry of the output thickness. The profile of the input thickness $h^{in}(x,y)$ is parameterized analogously using the coefficients $\bar{h}_i^{in}$ and Δh_i^{in}, $i = 1,\dots,N_P$.

4.2. Approximation of the plastic strain

The mathematical model of the camber formation expects the plastic strain parameterized as polynomial (cf. (10)). However, the use of the parameterization of the input and output thickness according to (11) does not yield a polynomial strain (cf. (1)). Therefore, the plastic strain (1) is approximated by the polynomial representation (10) using a weighted residuals method, see, e.g., [17]. To this end, the residual

$$\mathcal{R} = \left(\frac{h^{in}(x,y)}{h^{out}(x,y)} - 1\right) - \underbrace{\sum_{i=0}^{P_x}\sum_{k=0}^{P_y} c_{i,k} x^i y^k}_{\boldsymbol{\lambda}^{\mathrm{T}}(x,y)\mathbf{c}}$$

is forced to vanish in a weighted integral sense, i.e.,

$$\iint_{\Omega} \lambda(x,y)\mathcal{R}\,\mathrm{d}x\mathrm{d}y = 0. \tag{12}$$

The weighting function is denoted by $\lambda(x,y)$ and the integration domain Ω is the area of the plate as seen in Fig. 5. The coefficients $c_{i,k}$ of the polynomial plastic strain are arranged in the vector $\mathbf{c}$ and the vector $\boldsymbol{\lambda}(x,y)$ contains the corresponding terms $x^i y^k$. Additionally, it is required that (12) vanishes for each element of $\boldsymbol{\lambda}$ used as weighting function $\lambda(x,y)$. This approach yields the coefficient vector $\mathbf{c}$ as solution of the linear equation

$$\mathbf{A}\mathbf{c} = \mathbf{b} \tag{13}$$

with the matrix

$$\mathbf{A} = \iint_{\Omega} \boldsymbol{\lambda}\boldsymbol{\lambda}^{\mathrm{T}}\,\mathrm{d}x\mathrm{d}y \tag{14}$$

Post-print version of the article: F. Schausberger, A. Steinböck, and Kugi, "Optimization-based reduction of contour errors of heavy plates in hot rolling", *Journal of Process Control*, vol. 47, pp. 150–160, 2016, ISSN: 0959-1524. DOI: 10.1016/j.jprocont.2016.09.010
The content of this post-print version is identical to the published paper but without the publisher's final layout or copy editing.

and the vector

$$\mathbf{b} = \iint_{\Omega} \left(\frac{h^{in}(x,y)}{h^{out}(x,y)} - 1 \right) \boldsymbol{\lambda} \mathrm{d}x\mathrm{d}y. \tag{15}$$

The numerical properties of (13) are of good nature iff the components of $\boldsymbol{\lambda}$ are linearly independent because then $\mathbf{A}$ is positive definite. The integrations are performed analytically in (14) and by means of Gaussian quadrature in (15).

4.3. Formulation of the optimization problem

In the following, the asymmetry of the output thickness Δh_i^{out}, $i = 1, \ldots, N_P$ is used to reduce the occurring camber. The coefficients $\bar{h}_i^{out}$ of the center-thickness are set to the desired thickness value h_{des}^{out}, i.e., $\bar{h}_i^{out} = h_{des}^{out}$. Additionally, the profile of the input thickness $h^{in}(x,y)$ has to be known. Measurements of the input thickness profile are not available in every pass at the considered rolling mill. This is because there is only a thickness measurement device located downstream the rolling mill and the thickness over the whole plate is only measured after the last pass in the standard production process. Hence, instead of using measurements to determine the coefficients $\bar{h}_i^{in}$ of the center-thickness, they are set to the desired plate thickness of the previous pass. The asymmetry of the input thickness characterized by Δh_i^{in}, $i = 1, \ldots, N_P$ can by estimated based on the mathematical model from Section 3, see, [18]. In [18], the asymmetry of the output thickness of the previous pass is determined from the contour before and after the previous pass. However, in this paper the asymmetry of the input thickness is taken to be the desired asymmetry of the output thickness of the previous pass. The input thickness of the first controlled pass is considered to be homogeneous.

In the sequel, the centerline of the plate as shown in Fig. 6 is parameterized by $\delta(x)$ and is used as an aggregate measure of the two contours. The centerline of the plate before the roll pass $\delta^{in}(x)$ is calculated in the form (see Fig. 5)

$$\delta^{in}(x) = \frac{p_{B1}(x) + p_{B3}(x)}{2},$$

with the polynomials $p_{B1}(x)$ and $p_{B3}(x)$ of degree N_{PB} of the longitudinal edges of the plate. The centerline of the plate $\delta^{out}(x)$ after the roll pass follows as (cf. Fig. 6)

$$\delta^{out}\left(x + u(x, \delta^{in}(x))\right) = \delta^{in}(x) + v(x, \delta^{in}(x)),$$

with the displacements $u(x,y)$ and $v(x,y)$ from (9).

The asymmetry of the output thickness Δh_i^{out} is determined by solving the optimization problem

$$\min_{\Delta \mathbf{h}^{out} \in \mathbb{R}^{N_P}} V(\Delta \mathbf{h}^{out}) \tag{16}$$

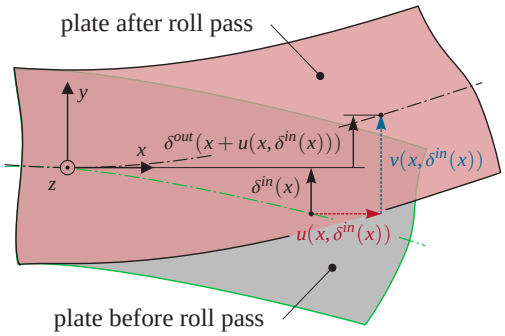

Figure 6: Centerline of the plate before and after the roll pass.

with the objective function

$$V(\Delta \mathbf{h}^{out}) = \frac{1}{M_{CL}} \sum_{j=1}^{M_{CL}} \left(\delta_{des}(x_j) - \delta^{out}(x_j)\right)^2 + \frac{\beta_1}{N_P} \sum_{i=1}^{N_P} (\Delta h_i^{out})^2$$

$$+ \frac{\beta_2}{N_P - 1} \sum_{i=1}^{N_P - 1} \left(\Delta h_{i+1}^{out} - \Delta h_i^{out}\right)^2 + \frac{\beta_3}{N_P} \sum_{i=1}^{N_P} P\left(\Delta h_i^{out}\right)$$

$$= \mathbf{e}^{\mathrm{T}} \mathbf{e}. \tag{17}$$

Here, the desired centerline is denoted by $\delta_{des}(x)$ and M_{CL} is the number of values used for evaluating the centerline deviation $\delta_{des}(x) - \delta^{out}(x)$ on an equally spaced grid x_j, $j = 1, \ldots, M_{CL}$. Note that (17) is a sum of squares and can be written as $V(\Delta \mathbf{h}^{out}) = \mathbf{e}^{\mathrm{T}} \mathbf{e}$ with the vector $\mathbf{e}$. In general, the aim is a straight centerline, i.e., $\delta_{des} = 0$. The grid-point values of the asymmetry of the output thickness are the optimization variables and are arranged in the vector

$$\Delta \mathbf{h}^{out} = \begin{bmatrix} \Delta h_1^{out} & \Delta h_2^{out} & \ldots & \Delta h_{N_P}^{out} \end{bmatrix}^{\mathrm{T}}.$$

Beside weighting the difference between the desired and the simulated centerline, the positive constants β_1 and β_2 are used to weight the asymmetry of the output thickness and the change of the output asymmetry, respectively. The weighting factor β_2 may be used to account for the limited velocity of the mill actuators which change the roll gap asymmetry. The term $\beta_3 / N_P \sum_{i=1}^{N_P} P\left(\Delta h_i^{out}\right)$ with $\beta_3 > 0$ penalizes asymmetries outside the allowed range $\Delta h_i^{out} \in [\Delta h_{min}^{out}, \Delta h_{max}^{out}]$, where the penalty function

$$P(\Delta h_i^{out}) = \begin{cases} \left(\Delta h_i^{out} - \Delta h_{min}^{out}\right)^2 & \text{if } \Delta h_i^{out} < \Delta h_{min}^{out} \\ \left(\Delta h_i^{out} - \Delta h_{max}^{out}\right)^2 & \text{if } \Delta h_i^{out} > \Delta h_{max}^{out} \\ 0 & \text{else} \end{cases}$$

is used to form a soft constraint, see, e.g., [19]. Because of this soft-constraint formulation, it is not ensured that the constraints $\Delta h_{min}^{out} \leq \Delta h_i^{out} \leq \Delta h_{max}^{out}$ are exactly fulfilled. However, a properly chosen weighting factor β_3 keeps the violation of the constraints in an acceptable range.

Post-print version of the article: F. Schausberger, A. Steinböck, and Kugi, "Optimization-based reduction of contour errors of heavy plates in hot rolling", *Journal of Process Control*, vol. 47, pp. 150–160, 2016, ISSN: 0959-1524. DOI: 10.1016/j.jprocont.2016.09.010

4.4. Numerical solution of the optimization problem

The optimization problem (16) is solved using the Gauss-Newton method. This method features a superlinear convergence rate (cf. [19]) which facilitates short optimization times. The Gauss-Newton method requires only the evaluation of the Jacobian $\mathbf{J}(\Delta\mathbf{h}^{out})$ of the vector $\mathbf{e}$ in every iteration but not the Hessian $\mathbf{H}$ of the objective function. This is favorable in terms of computational effort. The Gauss-Newton method proved to be useful for the considered optimization problem. The iterative procedure to solve the optimization problem (16) proceeds as follows:

Step 0: Choose initial guess for $\Delta\mathbf{h}^{out}$.

Step 1: Compute the search direction $\mathbf{d} = -\left(\mathbf{J}^{\mathrm{T}}(\Delta\mathbf{h}^{out})\mathbf{J}(\Delta\mathbf{h}^{out})\right)^{-1}\mathbf{J}^{\mathrm{T}}(\Delta\mathbf{h}^{out})\mathbf{e}$ according to the Gauss-Newton method.

Step 2: Perform a line search, i.e. solve $\min_{\alpha\geq 0} V(\Delta\mathbf{h}^{out}+\alpha\mathbf{d})$ and apply the update $\Delta\mathbf{h}^{out} \leftarrow \Delta\mathbf{h}^{out}+\alpha\mathbf{d}$.

Step 3: If any termination criterion (maximum number of iterations, convergence) is fulfilled, stop here.

Step 4: Start again at Step 1.

The Jacobian $\mathbf{J}(\Delta\mathbf{h}^{out})$ of the vector $\mathbf{e}$ results as

$$\mathbf{J}(\Delta\mathbf{h}^{out}) = (\nabla\mathbf{e})^{\mathrm{T}}.$$

In Step 2, a line search based on a quadratic interpolation of the objective function evaluated along the search direction

$$V(\Delta\mathbf{h}^{out}+\alpha\mathbf{d}) \approx a_0 + a_1\alpha + a_2\alpha^2, \qquad (18)$$

with coefficients a_0, a_1 and a_2, is performed. The coefficients (polynomial) follow as

$$a_0 = V_0, \quad a_1 = -3V_0 - V_1 + 4V_{0,5}, \quad a_2 = 2V_0 + 2V_1 - 4V_{0,5}$$

with the abbreviation $V_\alpha = V(\Delta\mathbf{h}^{out}+\alpha\mathbf{d})$. The optimal step length α^* that minimizes the polynomial approximation (18) is calculated in the form

$$\alpha^* = \frac{1}{4}\frac{3V_0 + V_1 - 4V_{0,5}}{V_0 + V_1 - 2V_{0,5}}.$$

The optimal step length α^* is limited to $0 \leq \alpha^* \leq 1$ to avoid step lengths outside the interpolation range $0 \leq \alpha \leq 1$ in (18). Clearly, $a_2 > 0$ must be satisfied so that α^* is the minimum of the right-hand side of (18). Furthermore, the line search should ensure that $V(\Delta\mathbf{h}^{out}+\alpha^*\mathbf{d}) < V(\Delta\mathbf{h}^{out})$, i.e., the value of the objective function decreases in the current iteration. If $a_2 < 0$ or $V(\Delta\mathbf{h}^{out}+\alpha^*\mathbf{d}) > V(\Delta\mathbf{h}^{out})$, the entries of the search direction vector are halved, i.e. $\mathbf{d} \leftarrow 0.5\mathbf{d}$ and the line search is performed once again.

Three termination criteria are used in Step 3 to identify if the current solution $\Delta\mathbf{h}^{out}$ is acceptable:

- The entries of the vector of the search direction are sufficiently small, i.e., $\|\mathbf{d}\|_\infty < \gamma_x$ with the constant $\gamma_x > 0$.
- The value of the objective function is small enough, i.e., $V(\Delta\mathbf{h}^{out}) < \gamma_V$ with the tuning parameter $\gamma_V > 0$.
- The improvement of the objective function along the current search direction is smaller than the constant $\gamma_{dV} > 0$, i.e., $|V(\Delta\mathbf{h}^{out}) - V(\Delta\mathbf{h}^{out}+\alpha^*\mathbf{d})| < \gamma_{dV}$.

5. Asymmetric mill stand compliance

Generally, the compliance of the mill stand is not strictly symmetric, which can cause an asymmetric deflection in the lateral direction and hence a cambered plate if not considered. The effect of this imperfection is analyzed by means of the evolution of the centerline of a plate rolled with zero control action at the reversing mill stand of AG der Dillinger Hüttenwerke, Germany. As shown in Fig. 7, the maximum lateral deviation δ_{max} of the centerline of the plate (cf. Fig. 4) is unacceptably large, although the asymmetry is kept constant. The first passes show a positive camber, while δ_{max} becomes negative in the last pass ending up with $\delta_{max} \approx -20\,\mathrm{cm}$. Similar evolutions of the centerline have been observed for many other rolled plates without camber correction. This behavior, which is different

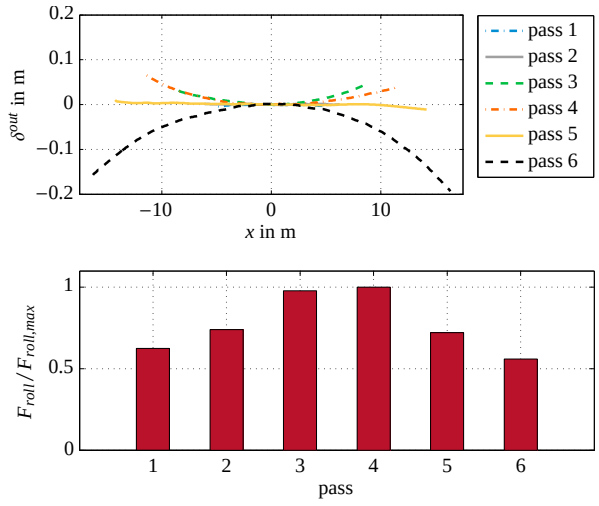

Figure 7: Measured evolution of the centerline for $\Delta\mathbf{h}^{out} = \mathbf{0}$ and averages of the measured normalized rolling force.

in consecutive roll passes, is assumed to be linked with the respective rolling force. Hence, a change of the rolling force from one pass to the next pass leads to an (additional) asymmetry of the output thickness. For the considered plate, the averages of the measured total rolling force are shown in the lower part of Fig. 7. Clearly, such imperfections jeopardize the effectivity of the control approach.

5.1. Compensation of the asymmetric mill stand deflection

To analyze the asymmetric deflection of the mill stand, the disturbance of the thickness asymmetry as a function of the

Post-print version of the article: F. Schausberger, A. Steinböck, and Kugi, "Optimization-based reduction of contour errors of heavy plates in hot rolling", *Journal of Process Control*, vol. 47, pp. 150–160, 2016, ISSN: 0959-1524. DOI: 10.1016/j.jprocont.2016.09.010
The content of this post-print version is identical to the published paper but without the publisher's final layout or copy editing.

rolling force needs to be known. During a measurement campaign, additional to the thickness measurement after the last pass, the thickness profile of the plate was measured after every forward pass. The thickness asymmetry of the plate after the backward pass was determined using the estimation approach presented in [18]. In this approach, the estimated contour before and after the considered rolling pass is used to estimate the output thickness asymmetry after the pass. The necessary input asymmetry is determined using thickness measurements after the previous pass. Based on the determined thickness asymmetries of different plates, an almost linear relation between the output thickness asymmetry and the applied rolling forces has been observed. Hence, the disturbance Δh_{dist}^{out} of the thickness asymmetry is empirically formulated as

$$\Delta h_{dist}^{out} = \begin{cases} \frac{w}{w_{cyl}} \Delta h_0 + k_F \frac{w}{w_{cyl}} F_{roll} & \text{in forward passes} \\ \frac{w}{w_{cyl}} \Delta h_0 + k_B \frac{w}{w_{cyl}} F_{roll} & \text{in backward passes,} \end{cases}$$

with the compliance constants k_F and k_B for rolling passes in the forward and backward direction, respectively. Furthermore, Δh_0 denotes an unknown offset of the asymmetry and w_{cyl} is the lateral distance between the cylinders of the roll gap actuator. The term w/w_{cyl} maps the asymmetric deflection of the mill stand to the output asymmetry of the plate. The deflection constants were identified as $k_F = 15.0\,\mu\text{m/MN}$ and $k_B = 17.4\,\mu\text{m/MN}$ utilizing measurements of different plates and the least-squares method. The constants k_F and k_B mainly depend on the mechanical properties of the mill stand housing. Hence, they have to be determined only once in the course of a calibration process unless the mechanical setup of the mill stand housing is significantly changed.

The value of Δh_0 may change because after every change of the work rolls a calibration routine affecting Δh_0 is performed. Here, the tilt of the rolls is manually adjusted to yield a symmetric roll gap profile. Furthermore, the operator of the mill stand may change the tilt during the roll process. Therefore, the compensation is done relatively to the deflection caused by a reference rolling force $F_{roll,ref}$ (cf. Fig. 8).

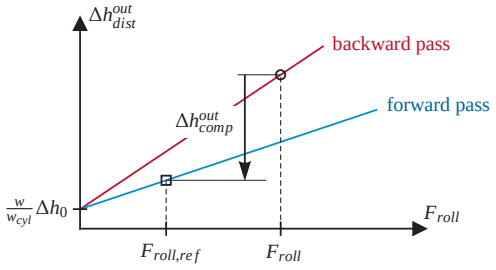

Figure 8: Compensation of the asymmetric deflection of the rolling mill relative to the reference rolling force $F_{roll,ref}$ stemming from a forward pass.

The rolling force F_{roll} before the first controlled pass is used as $F_{roll,ref}$. If $F_{roll,ref}$ stems from a backward pass, the compensation Δh_{comp}^{out} reads as

$$\Delta h_{comp}^{out} = \begin{cases} \frac{w}{w_{cyl}} \left(k_B F_{roll,ref} - k_F F_{roll} \right) & \text{in forward passes} \\ \frac{w}{w_{cyl}} k_B \left(F_{roll,ref} - F_{roll} \right) & \text{in backward passes,} \end{cases}$$

or is calculated in the form

$$\Delta h_{comp}^{out} = \begin{cases} \frac{w}{w_{cyl}} k_F \left(F_{roll,ref} - F_{roll} \right) & \text{in forward passes} \\ \frac{w}{w_{cyl}} \left(k_F F_{roll,ref} - k_B F_{roll} \right) & \text{in backward passes,} \end{cases}$$

if $F_{roll,ref}$ stems from a pass in forward direction. The vector of the required values of the roll gap asymmetry $\mathbf{\Delta h}_{req}^{out}$ results as

$$\mathbf{\Delta h}_{req}^{out} = \mathbf{\Delta h}^{out} + \begin{bmatrix} 1 & \dots & 1 \end{bmatrix}^{\mathrm{T}} \Delta h_{comp}^{out}. \tag{19}$$

The values contained in $\mathbf{\Delta h}_{req}^{out}$ are sent to the automation system of the rolling mill before every roll pass. Hence, the desired rolling forces are used in the compensation approach.

6. Simulation results

The following section shows simulation results of the proposed method. To this end, the evolution of the contour is predicted using the mathematical model from Section 3. The simulated contour is used in the optimization-based approach from Section 4 to determine the required output thickness profile of the next pass. Besides contour errors resulting from upstream processes (e.g. casting process, roughing mill), generally unknown, non-homogeneous input profiles constitute common imperfections before the first pass on the considered rolling mill. Hence, an asymmetric input profile and an initial contour error at the beginning of the rolling are used to validate the control approach. An ideal roll gap actuator was assumed in the derivation of the control concept. Under real rolling conditions, position control of the roll gap may be imperfect. Hence, the effect of deviations between the required and the actual output asymmetry are investigated. Because no model of the mill stand compliance is used in the simulations, the effect of the asymmetric mill stand deflection is not considered in the simulations.

Table 1: Parameters used for the computations.

Parameter	Value	Unit
N_P	15	
P_x	20	
P_y	4	
N_{PB}	4	
M_{CL}	100	
γ_x	10^{-7}	m
γ_V	10^{-8}	m^2
γ_{dV}	10^{-7}	m^2
β_1	10	
β_2	10^4	
β_3	10^4	
Δh_{min}^{out}	-0.3	mm
Δh_{max}^{out}	0.3	mm

Post-print version of the article: F. Schausberger, A. Steinböck, and Kugi, "Optimization-based reduction of contour errors of heavy plates in hot rolling", *Journal of Process Control*, vol. 47, pp. 150–160, 2016, ISSN: 0959-1524. DOI: 10.1016/j.jprocont.2016.09.010

The parameters used in the simulations are shown in Tab. 1 and their actual choice is outlined in the following. The number of grid points $N_P = 15$ used to define the thickness profiles is predefined by the automation system of the rolling mill. The polynomial degree P_x should be larger than N_P to yield a sufficient approximation of the plastic strain in the longitudinal direction. However, a too large value of P_x leads to an extensive computational effort. For the considered application, $P_x = 20$ has been found to be a good compromise. The same argumentation holds true for the degree $P_y = 4$ in the lateral direction where a more or less linear profile has to be approximated. The degree of the boundary polynomials $N_{PB} = 4$ ensures a sufficiently accurate approximation of the boundaries of the plate while still keeping the computational effort acceptable. M_{CL} as the number of values used for evaluating the centerline deviation should be a multiple of N_P so that several values of the centerline between neighboring grid points of the thickness profile are contained in the objective function. The constants γ_x, γ_V and γ_{dV} used in the different termination criteria were determined by means of simulation studies such that a good convergence of the Gauss-Newton method with a tolerable number of iterations is ensured.

The weighting factors β_1, β_2, and β_3 specifically influence the control behavior. Their actual choice was determined by means of a simulation of a representative rolling pass. In particular, the last rolling pass of a long and thin plate was chosen for the simulation because for such plates camber plays an important role. First, the simulation was performed with all three weighting factors set to zero, i.e., $\beta_1 = \beta_2 = \beta_3 = 0$. Then the weighting factor β_1 which penalizes the asymmetry of the output thickness was increased beginning from a small value (10^{-5}) until the desired control behavior was achieved. Here, a satisfying result was obtained for $\beta_1 = 10$. The same procedure was performed for the weighting factor β_2 which penalizes the change of the output asymmetry along the length of the plate. The aim was a sufficiently homogeneous thickness asymmetry, which was obtained for $\beta_2 = 10^4$. The constant β_3 was increased until the violation of the constraints Δh^{out}_{min} and Δh^{out}_{max} was sufficiently small. In addition to the role of β_1 as weighting factor in the objective function, a large value of β_1 contributes to a good-natured optimization problem due to the regularizing effect of the term $\beta_1/N_P \sum_{i=1}^{N_P} (\Delta h_i^{out})^2$, see, e.g., [19]. The weighting factors β_1, β_2, and β_3 may be changed for different materials and dimensions of the rolled plates. However, for the considered application constant parameters have led to satisfying control results for the whole product range.

In the simulations, a plate with initial length $l = 6.92\,\mathrm{m}$ and width $w = 2.59\,\mathrm{m}$ and an initial thickness $h = 60.2\,\mathrm{mm}$ is considered. At the end of the rolling process, a final plate length of 31.7 m and a final plate thickness of 13.1 mm should be achieved. The production schedule of the considered plate is shown in Tab. 2.

Table 2: Production schedule of the simulated rolling process.

pass	1	2	3	4	5	6
h^{out}_{des} in mm	48.1	36.3	26.2	18.8	15.1	13.1

6.1. Initial input thickness asymmetry

In the first simulation, an asymmetric plate thickness ($\Delta h^{in} = -1\,\mathrm{mm}$) and a rectangular plate contour are assumed before the first considered pass. Such thickness asymmetries in combination with a rectangular plate may result from the lateral spreading (rolling in the width direction) of the plate at the roughing mill stand. The initial thickness profile is not known by the camber reduction approach. The resulting centerline of the plate after each pass and the control effort resulting from solving the optimization problem (16) are shown in Fig. 9. Due to the initial rectangular contour and the unknown input profile of the plate, no control action is performed in the first pass, i.e. $\Delta h^{out}_{req,1} = 0$. This causes a cambered plate after the first pass because of the non-homogeneous deformation. The camber is successively reduced to almost zero in the subsequent passes. Without constraints regarding the asymmetry and with setting $\beta_1 = 0$, i.e. no weighting of the asymmetry in the objective function $V(\mathbf{\Delta h}^{out})$, the contour error resulting after pass 1 would be compensated after the next pass. A non-homogeneous thickness profile remains in the lateral direction after the last roll pass, which is caused by the initial thickness asymmetry.

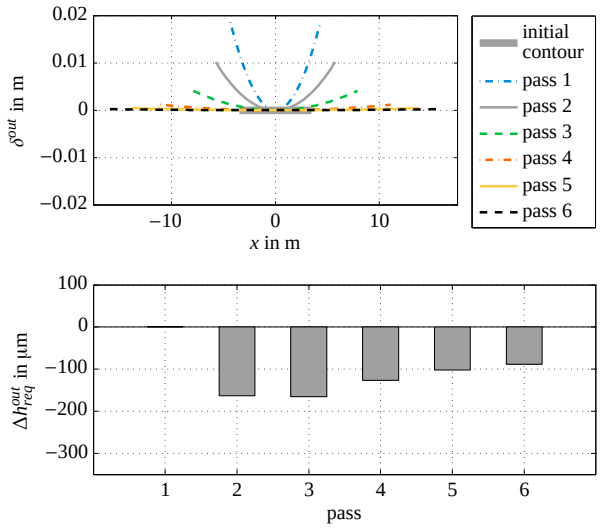

Figure 9: Simulation results for an initial asymmetry of the input thickness $\Delta h^{in} = -1\,\mathrm{mm}$.

6.2. Initial contour error

In the second simulation study (cf. Fig. 10), a contour error with a homogeneous thickness distribution at the beginning of the roll passes is assumed. Here, the constraint Δh^{out}_{min} on the asymmetry of the output thickness is active in the first three passes. Without constraints and with $\beta_1 = 0$ the initial contour error would be compensated within a single pass. However, after a few passes the contour error is reduced to an acceptable range at the cost of an asymmetric thickness profile after the last roll pass.

Post-print version of the article: F. Schausberger, A. Steinböck, and Kugi, "Optimization-based reduction of contour errors of heavy plates in hot rolling", *Journal of Process Control*, vol. 47, pp. 150–160, 2016, ISSN: 0959-1524. DOI: 10.1016/j.jprocont.2016.09.010

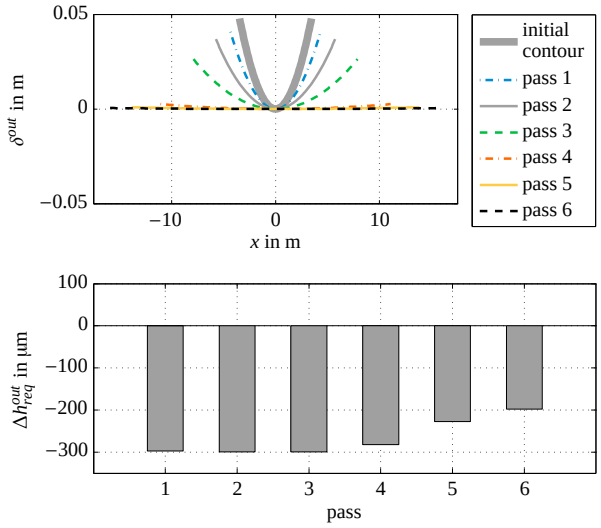

Figure 10: Simulation results for an initial contour error.

6.3. Non-ideal actuator position control

The last simulation covers both, an unknown asymmetric input thickness profile ($\Delta h^{in} = -1\,\text{mm}$) and a known cambered plate before the first pass. Furthermore, a ratio of $\kappa = \Delta h^{out}_{act}/\Delta h^{out}_{req} = 0.5$ between the actual and the required asymmetry due to an inaccurate actuator is assumed.

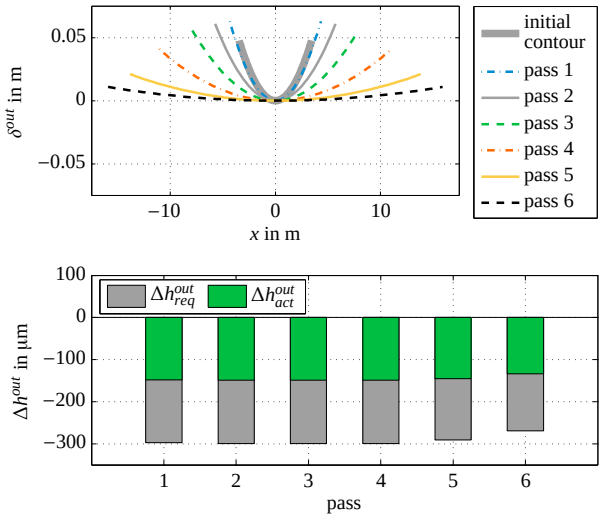

Figure 11: Simulation results for an initial input thickness wedge and a contour error. Furthermore, a non-ideal position control of the roll gap actuator is considered.

Even for this simulation scenario, the camber of the plate can be successively reduced in the simulated rolling passes as can be seen in Fig. 11. However, the centerline of the plate after the last roll pass shows a small but acceptable camber. A ratio of $\kappa > 1$ also results in a successful reduction of the camber. Clearly, $\kappa > 1$ yields an overcompensation of the camber and hence causes an oscillation of the centerline about $\delta^{out} = 0$. In practical terms, the considered imperfection of the roll gap actuators deteriorate the control result only slightly, because $\kappa \approx 1$ holds under real rolling conditions due to the compensation of the asymmetric deflection of the mill stand.

7. Experimental results from industrial implementation

In the following, results obtained for a plate rolled at the reversing mill stand of AG der Dillinger Hüttenwerke with the proposed camber reduction strategy are presented. The parameters listed in Tab. 1 were used and the production schedule is the same as in Section 6 (cf. Tab. 2). The algorithms for the estimation of the plate contour and for the optimization-based reduction of contour errors were implemented in C++. The convergence criteria of the optimization problem (16) are typically fulfilled within 3 iterations resulting in computing times of approximately 20 ms to solve the optimization problem (Standard PC with i7-2600 @ 3.4 GHz processor and 16 GB RAM).

Two infrared cameras are installed at the ceiling of the considered rolling mill. One camera was mounted in front of the rolling mill to measure the outgoing contour in backward passes. The second camera is located behind the rolling mill to capture the outgoing plate contour in the forward pass. Hence, a measurement of the plate contour is available after every pass. As shown in Fig. 12, the estimated contour of the forward pass is used to calculate the required asymmetry of the output thickness characterized by the vector $\mathbf{\Delta h}^{out}_{req}$ for the consecutive backward pass. Consequently, the measured contour of the backward pass determines the target value of the output thickness for the following forward pass, and so on.

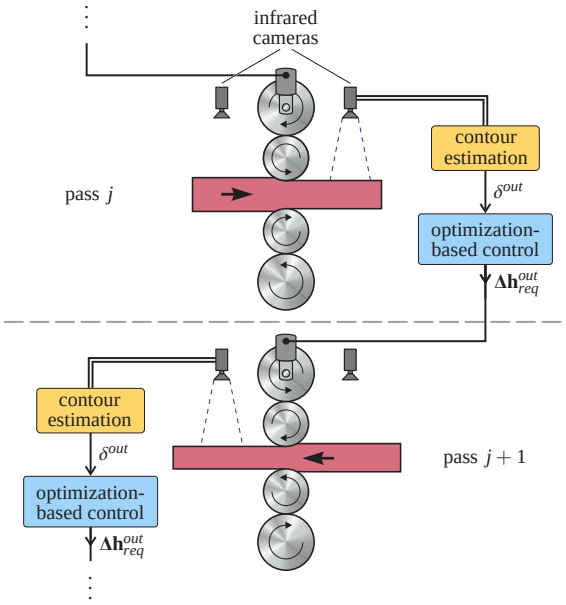

Figure 12: Schematic of the contour estimation in combination with the proposed method for the reduction of contour errors.

Fig. 13 shows the evolution of the centerline with applying the proposed method for the reduction of contour errors and the compensation of the asymmetric mill stand deflection according to (19). Note that the geometrical properties of the rolled

Post-print version of the article: F. Schausberger, A. Steinböck, and Kugi, "Optimization-based reduction of contour errors of heavy plates in hot rolling", *Journal of Process Control*, vol. 47, pp. 150–160, 2016, ISSN: 0959-1524. DOI: 10.1016/j.jprocont.2016.09.010
The content of this post-print version is identical to the published paper but without the publisher's final layout or copy editing.

plate are similar to the plate from Fig. 7. This facilitates a comparison between the obtained results. Additionally, the normalized asymmetry of the output thickness resulting from solving the optimization problem (16) and the compensation of the mill stand deflection, as well as the required total asymmetry of the output thickness are shown. Again, the chosen weights cause an almost constant asymmetry along the length of the plate. This allows the use of a scalar value Δh^{out} which is independent of the longitudinal coordinate x of the plate, see Fig. 13. Furthermore, the normalized desired rolling forces are shown in the lower part of the figure.

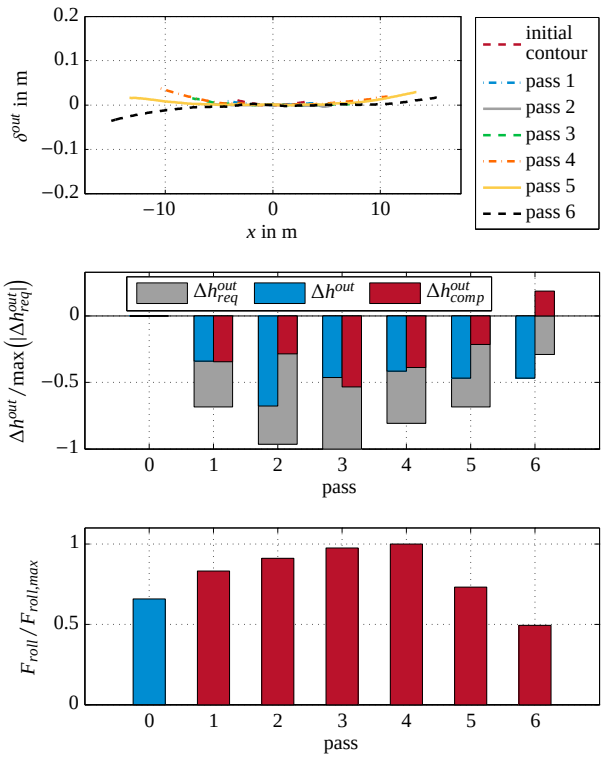

Figure 13: Measurement results of a rolled plate with active camber control and the compensation of the asymmetric deflection of the mill stand.

The centerline after each pass and (more important) after the last pass is close to the desired value $\delta^{out}_{des} = 0$. Due to the decreasing rolling forces in the last two passes, the compensation of the deflection has a significant influence on the required asymmetry. After the first two passes, the necessary control effort Δh^{out} remains nearly constant.

8. Conclusions and outlook

In this work, an optimization-based approach for the reduction of contour errors occurring during the rolling of heavy plates was developed. First, a vision-based method for the measurement of the plate contour was shortly revisited and a continuum-mechanics-based mathematical model of the contour evolution of the plate was discussed. The mathematical model predicts the contour after the roll pass based on the contour before the roll pass and the input and output thickness profiles. Using a tailored parameterization of the thickness profiles, this model serves as a basis for the optimization-based approach for the reduction of contour errors. The optimization problem allows to systematically incorporate constraints on the asymmetry of the output thickness and is solved using the Gauss-Newton method.

An empirical compensation of the asymmetric deflection of the mill stand was presented. This helps to reduce disturbing effects due to changes of the rolling force. Furthermore, the results of different simulation scenarios demonstrate that the proposed method effectively reduces contour errors. Measurement results from a plate rolled at AG der Dillinger Hüttenwerke indicate that the contour error can be significantly reduced.

It is planned to apply the presented methods in a feedback control approach to minimize the delay between contour measurement and camber correction, which should further reduce contour errors, in particular in the last roll pass. To this end, the control system has to be adapted to allow for an adjustment of the roll gap asymmetry during the pass.

Acknowledgements

The authors gratefully acknowledge ongoing support and the realization of the measurements by AG der Dillinger Hüttenwerke, Germany. The second author gratefully acknowledges financial support provided by the Austrian Academy of Sciences in the form of an APART-fellowship at the Automation and Control Institute of TU Wien.

References

[1] T. Ishikawa, Y. Tozawa, and J. Nishizawa. Fundamental study on snaking in strip rolling. *Trans. Iron Steel Inst. Jpn.*, 28(6):485–490, 1988.

[2] T. Shiraishi, H. Ibata, A. Mizuta, S. Nomura, E. Yoneda, and K. Hirata. Relation between camber and wedge in flat rolling under restrictions of lateral movement. *Iron Steel Inst. Jpn. Int.*, 31(6):583–587, 1991.

[3] A. Dixon and D. Yuen. Mathematical analysis of the effects of widthwise asymmetric rolling conditions on head-end wedge, camber and off-centre. In *Rolling 2013 - 9th Int. Rolling Conf. and the 6th European Rolling Conf.*, Venice, Italy, June 2013.

[4] D. L. Biggs, S. J. Hardy, and K. J. Brown. Finite element modelling of camber development during hot rolling of strip steel. *Ironmak. and Steelmak.*, 25(1):81–89, 1998.

[5] A. Nilsson. FE simulations of camber in hot strip rolling. *J. Mater. Proc. Tech.*, 80–81:325–329, 1998.

[6] M. Trull, D. McDonald, A. Richardson, and D. C. J. Farrugia. Advanced finite element modelling of plate rolling operations. *J. Mater. Proc. Tech.*, 177:513–516, 2006.

[7] T. Kiyota, H. Matsumoto, Y. Adachi, E. Kondo, Y. Tsuji, and S. Aso. Tail crash control in hot strip mill by LQR. In *Proceedings of the American Control Conference*, pages 3049–3054, Denver, Colorado, June 2003.

[8] M. Okada, K. Murayama, Y. Anabuki, and Y. Hayashi. VSS control of strip steering for hot rolling mills. In *Proceedings of the 16th IFAC World Congress*, pages 1681–1686, Prague, Czech Republic, July 2005.

[9] I. Choi, J. Rossiter, J. Chung, and P. Fleming. An MPC strategy for hot rolling mills and applications to strip threading control problems. In *Proceedings of the 17th IFAC World Congress*, pages 1661–1662, Seoul, Korea, July 2008.

[10] I. Malloci, J. Daafouz, C. Iung, R. Bonidal, and P. Szczepanski. Robust steering control of hot strip milling. *IEEE Trans. on Control Systems Technol.*, 18(4):908–917, 2010.

Post-print version of the article: F. Schausberger, A. Steinböck, and Kugi, "Optimization-based reduction of contour errors of heavy plates in hot rolling", *Journal of Process Control*, vol. 47, pp. 150–160, 2016, ISSN: 0959-1524. DOI: 10.1016/j.jprocont.2016.09.010
The content of this post-print version is identical to the published paper but without the publisher's final layout or copy editing.

[11] Y. Tanaka, K. Omori, T. Miyake, K. Nishizaki, M. Inoue, and S. Tezuka. Camber control techniques in plate rolling. Technical Report 16, Kawasaki Steel, June 1987.

[12] D. Jeong, Y. Kang, Y. J. Jang, D. Lee, and S. Won. Development of FEM simulator combined with camber reducing output feedback fuzzy controller for rough rolling process. *Iron Steel Inst. Jpn. Int.*, 53(3):511–519, 2013.

[13] F. Schausberger, A. Steinboeck, and A. Kugi. Optimization-based estimator for the contour and movement of heavy plates in hot rolling. *J. Process Control*, 29:23–32, 2015.

[14] F. Schausberger, A. Steinboeck, and A. Kugi. Mathematical modeling of the contour evolution of heavy plates in hot rolling. *Appl. Math. Modell.*, 39(15):4534–4547, 2015.

[15] M. H. Sadd. *Elasticity, Theory, Applications and Numerics*. Academic Press, Burlington, 2nd edition, 2009.

[16] A. Kugi, W. Haas, K. Schlacher, K. Aistleitner, H.M. Frank, and G.W. Rigler. Active compensation of roll eccentricity in rolling mills. *IEEE Trans. Ind. Appl.*, 36(2):625–632, 2000.

[17] J. N. Reddy. *An Introduction to the Finite Element Method*. McGraw-Hill London, 3rd edition, 2006.

[18] F. Schausberger, A. Steinboeck, A. Kugi, M. Jochum, D. Wild, and T. Kiefer. Estimation of the thickness asymmetry using models for the contour evolution and vision-based measurements of plates in hot rolling. In *Proceedings of the METEC and 2nd ESTAD 2015*, pages 1–8, Düsseldorf, Germany, June 2015.

[19] J. Nocedal and S. J. Wright. *Numerical Optimization*. Springer Series in Operations Research. Springer, New York, 2nd edition, 2006.

Post-print version of the article: F. Schausberger, A. Steinböck, and Kugi, "Optimization-based reduction of contour errors of heavy plates in hot rolling", *Journal of Process Control*, vol. 47, pp. 150–160, 2016, ISSN: 0959-1524. DOI: 10.1016/j.jprocont.2016.09.010
The content of this post-print version is identical to the published paper but without the publisher's final layout or copy editing.